THE ASTRONOMICAL JOURNAL VOLUME 100, NUMBER 5 NOVEMBER 1990

GALAXY VELOCITIES AND SUBSTRUCTURES IN SOUTHERN CLUSTERS: A496 AND SERSIC 40/6, EXAMPLES OF DYNAMICAL CUSPS

H. QUINTANA[a),b)] AND A. RAMÍREZ[b)]
Astrophysics Group, Pontificia Universidad Católica de Chile, Casilla 6014, Santiago, Chile
Received 7 September 1989; revised 28 June 1990

ABSTRACT

Estimates of velocity dispersions, mean velocities, and virial masses are given for Sersic 40/6 and A496, based on new observations and published data of 84 and 70 galaxies, respectively. The main optical and x-ray structures together with the velocity field distributions of these clusters are briefly discussed. Both clusters show the presence of density cusps of approximately 0.2 Mpc radius around the central galaxies, having velocity dispersions significantly lower than the clusters overall values that blend smoothly with the cD halo dispersions. In A496 the core galaxies can be considered bound to the cD, forming a dynamical subunit. The core group around the central db in Sersic 40/6 has half its cluster measured dispersion. Although the core dispersion is high, it could be bound if the global high dispersion value is confirmed. An application of the virial theorem using the cD satellite galaxies gives masses of $\sim(2.1\pm1)\times10^{14}\,\mathscr{M}_\odot$ and $\sim(2.5\pm1)\times10^{12}\,\mathscr{M}_\odot$ for the cD galaxies in Sersic 40/6 and A496, respectively. Some consideration is given to the implication for theories of cD formation and evolution. Cooling flows can be affected by the presence of these central dynamical subunits in the inner regions where they control their flow.

I. INTRODUCTION

Studies of the dynamics and structure of galaxy clusters require extensive observational optical, x-ray, and radio data. Basic among the optical data are the determination of the galaxy velocities and magnitudes, morphological types, and number counts or positional information. Realistic models of cluster evolution must take into account the substructures as revealed by the intracluster gas, galaxy density, and velocity field distributions. Numerical simulations begin to allow detailed modeling of the interactions between the evolving galaxy, gas, and assumed dark matter components. A major uncertainty in all models stems from the presence of dark matter of unknown origin which may have a key influence on the formation and dynamical evolution of the structures.

Two strong x-ray clusters at southern declinations, which have been fairly well studied, are A496 and Sersic 40/6 (A3266 in the new catalog of Abell *et al.* 1989), for which we report here further optical data, obtained from spectroscopic observations at the du Pont telescope at Las Campanas Observatory and direct plates taken at Cerro Tololo Inter-American Observatory.

The cluster A496, a $R=2$ and BM = I: type cluster, has the second strongest detected cooling flow in its center (Nulsen *et al.* 1982), presenting an added observer's interest as it is at a higher galactic latitude than 0745 − 19, the strongest cooling flow detected cluster which lies in a very crowded star region. Previous optical studies of the velocity field of A496 were carried out by Quintana *et al.* (1985), who determined 32 velocities, by Proust *et al.* (1987), who measured 15 velocities (two new members), and by Hu *et al.* (1985), who obtained velocities of the central galaxy and three other very close companions. Moreover, Tonry (1985) measured the velocities and internal dispersions of the cD and of a close satellite and Green *et al.* (1988) obtained a further three velocities. We have observed an additional 34 new (and five repeated) galaxies, refining the determination of dynamical parameters for this cluster and getting a clearer picture of its velocity field and dynamical substructure. From counts down to 18 mag over an area covering a $5°\times5°$ field, we study the presence of possible density substructures at small and large scale around the cluster. Mazure *et al.* (1986) using data taken from Dressler's morphological catalog (1980), claimed to detect a density substructure to the south of the core of A496, but our counts show an elongation in the galaxy structure in a somewhat different direction. However, we detect in velocity space an outlying subgroup reported by them.

The cluster Sersic 40/6, $R=2$ and BM = I–II, was first dynamically studied by Melnick and Quintana (1981a and 1981b), who obtained 29 galaxy velocities. Later Materne *et al.* (1982) and Green *et al.* (1988) increased the total number of measured galaxy velocities to 33. Using a fiber-optics spectrograph Carter *et al.* (1984) obtained 29 redshifts and reported a velocity dispersion of 1410 km s^{-1}, but they give no individual velocities. Furthermore, Carter *et al.* (1985) obtained spectra along the line passing through both nuclei of the dumbbell in Sersic 40/6. Here we present 51 additional velocities confirming the high virial mass of this cluster and showing the presence of a dynamical subunit at the center. Galaxy counts reaching down to 18 mag in an area of $5°\times5°$ show the cluster to have a regular symmetric structure with small-scale inhomogeneities not apparent in the velocity field.

We draw attention, in particular, to the presence in both clusters of a tight group of faint galaxies surrounding the central galaxies, the cD in A496 and the supergiant db in Sersic 40/6 (a complex cD as well), forming a density cusp. A population of faint satellite galaxies around brightest cluster members (BCM's) was claimed to have been detected by Cowie and Hu (1986), using data from few galaxies close to BMC's in each of 14 rich clusters. Bower *et al.* (1988) ana-

[a)] Guest Observer at Las Campanas Observatory, Carnegie Institution of Washington, Washington, DC.
[b)] Visiting Astronomer at Cerro Tololo Inter-American Observatory, National Optical Astronomy Observatories, operated by the Association of Universities for Research in Astronomy, Inc., under contract with the National Science Foundation.

lyzed the velocities in the central region of the cD cluster A2029 and found no suggestion of a bound satellite group around the cD. However, Bothun and Schombert (1988) recently looked at three clusters and in only one of them found a satellite population with low velocity dispersion. In the other two clusters the apparent satellites had the cluster large velocity dispersion. We have found at least another cluster with a bound central population and a second where this is a possibility. The small relative velocity dispersion of these groups and the plausible assumption that they are bound to the central galaxies allow us to derive an estimate of the dynamical masses of these dominant galaxies. In future publications we will analyze the photometric and global structural properties of the distribution of galaxies in A496 and Sersic 40/6.

In Sec. II we describe the observations and data-reduction procedures. In Sec. III we present the velocities, velocity dispersions and distributions, number counts, and density maps obtained, while in Sec. IV we discuss results, derive dynamical masses, and evaluate the significance of substructures. Finally, in Sec. V we summarize our conclusions. When needed we have used a Hubble constant $H_0 = 50$ km s^{-1} Mpc^{-1}.

II. OBSERVATIONS AND DATA REDUCTION

Galaxies observed spectroscopically were chosen mainly in terms of decreasing brightness and distributed in such a way as to cover more or less homogeneously the clusters surfaces. In both targets we paid special attention to the group of galaxies surrounding the brightest member, reaching much fainter magnitudes than elsewhere. However, the observed samples are not magnitude complete and some fairly bright galaxies do not have a velocity measurement yet. Nevertheless, we expect the samples to be representatives of the whole clusters. The spectroscopic observations included in these results were made in four separate runs totaling 19 partial nights at the 100″ du Pont telescope of the Las Campanas Observatory, in April and December 1982, February 1983 and March 1984. We used the Boller and Chivens spectrograph with a 600 l/mm grating giving a useful range from 3500 Å to 7000 Å, with a resolution of 2 Å (2 pixels) on the Shectograph detector. This system employs a dual array of 936 diodes, which can be divided at read-out time in four pixel elements each, giving two rows 3744 pixel long (Shectman 1981). They are used to record spectra from two entrance apertures on the spectrograph, which we usually choose to be 2×4 arcsec on the sky. One of them admits starlight and sky background, the other only sky. Apertures were flipped two or three times between objects and sky. Typical exposures were 5–20 min depending on galaxy magnitude, compactness, and seeing. Comparison spectra were taken before and after each object sequence, which consisted in three or four exposures, at similar telescope position and from galaxies in the same cluster. Observations of 2–3 standard spectrophotometric stars each night, chosen from Stone and Baldwin (1983), were made to calibrate spectra in flux. Spectra of stars and bright galaxies with known velocities were also taken to evaluate external errors.

Reductions were carried out with the IRAF image-processing system on the VAX8600 of the Universidad Católica of Chile. Comparison spectra from a He–Ar lamp were calibrated with 5 or 6 order Legendre polynomials, using 16–25 spectral lines, giving a rms fit smaller than 0.3 Å. The accuracy was checked with the sky lines: [O I] 5577.35 Å, Na I 5891.95 Å, [O I] 6300.23 Å, and [O I] 6363.88 Å, where normally a deviation smaller than 0.4 Å per line was found. The wavelength calibration was performed separately for the upper and lower rows of the array, because a mean shift equivalent to 30 km s^{-1} was found between the upper and lower rows and when both spectrum were directly added a degradation of the line resolutions occurred. After wavelength calibration they could be combined without introducing additional errors.

In the normalized and flux calibrated spectra of each galaxy a Gaussian fit was made to all spectral lines (emission or absorption) to determine positions. Rest wavelengths were chosen from the list of elements that Sandage (1979) used to determine nearly 750 galaxy velocities. Redshifts were computed using a quadratic minimization of line velocities residuals of computer identified lines for each spectrum. From the measurement of 5–12 spectral lines, typically: H, K,Ca 4226 Å, G band, Hγ, Fe 4384 Å, Hβ, Mg triplet, Na, and occasionally emission in [O II] 3727 Å, [O III] 4959 and 5007 Å, and Hα lines, we obtained a typical rms error of the mean radial velocity of galaxies in the range 30–40 km s^{-1}. External velocity comparison showed good agreement with velocities of standard objects (stars and bright galaxies), implying that no zero-point correction in velocity was needed for this instrument. Table I shows the velocity differences between published and measured values for our chosen standard objects. In all cases the resulting velocities are within the range of expected values, even when we used for reference stars a line position list compiled for galaxy spectra. This would introduce a small additional error that explains the larger individual uncertainties obtained for the stars than for the reference galaxies. Standard velocity stars have a mean difference of 3 ± 6 km s^{-1}, standard velocity galaxies have -5 ± 18 km s^{-1}. The total sample of standard objects give a mean difference of -1 ± 9 km s^{-1}. These values imply that errors due to an instrument systematic effect are insignificant in our data and that a zero-point correction with respect to the chosen standards is negligible.

III. RESULTS

The individual heliocentric velocities of cluster galaxies are presented in Tables II and III for Sersic 40/6 and A496, respectively. In order to obtain the best estimates of the mean velocity (v) and velocity dispersion (σ_v) for each cluster we have included all previously published velocities found in the literature up to the end of 1988. The 84 galaxies of Sersic 40/6 originate: nine from Melnick and Quintana (1981a), 17 from Melnick and Quintana (1981b), two from Materne *et al.* (1982), one from Green *et al.* (1988), and 55 from the present work. The 70 galaxies of A496 originate: 29 from Quintana *et al.* (1985), two from Hu *et al.* (1985), one from Proust *et al.* (1987), and 38 from the present work. The velocity of the cD was taken as the average of measured and published values, because of the good data reported for this velocity. Column 1 gives an identification number (to be used in future papers on photometry). In Columns 2 and 3 we give the 1950.0 equatorial coordinates. For Sersic 40/6 these were determined from measurements made, with respect to 12 SAO stars, on the film copy of the ESO/SRC J-survey field 118 with an x-y encoded light table fitted with a microscope. We estimate the accuracy in these positions to be about ± 3 arcsec. Coordinates were determined for A496 from the glass copy of the Palomar Sky Survey, using the Optronics machine at ESO Garching with reference to 18

TABLE I. Heliocentric measured velocities of standard objects.

Object name (1)	Number of observations (2)	Number of lines (3)	$v_{\odot}(Obs.)^a$ (kms^{-1}) (4)	$v_{\odot}(Ref.)^b$ (kms^{-1}) (5)	Δv^c (kms^{-1}) (6)
HD22663	1	9	14± 10	11.4± 1.4	3± 10
HD23319	1	7	2± 20	10.7± 0.8	- 9± 20
HD38014	3	8	65± 23	55± 1	10± 23
HD95486	1	9	-49± 10	-55.9± 0.5	7± 10
NGC596	2	10	1919± 9	1902± 15	17± 18
NGC3309	7	9	4079± 5	4093± 43	-21± 43
NGC1700	1	8	3988± 15	3953± 31	35± 34
NGC1316	1	10	1750± 11	1801± 39	-51± 41

[a] Error is the standard deviation of the unweighted mean of individual lines for a spectrum or the unweighted mean of several spectra.
[b] Reference of velocities: Stars of spectral type K or G: Abt and Biggs (1972). Galaxies: Sandage and Tammann (1981).
[c] Error is the square root of squared sums of individual errors.

SAO stars. The accuracy in these later positions is about ± 1 arcsec, errors mostly due to visual centering of galaxies. Column 4 shows the number of lines used in the velocity measurements. Columns 5 and 6 give heliocentric velocities together with estimated internal errors. If more than one spectrum was available for a given galaxy, this error is the standard deviation of the unweighted mean of individual spectra. Columns 7 and 8 list the values from previous velocity measurements and Columns 9 and 10 give their reference sources and cross identification numbers. Column 11 in Table III shows the Dressler number as appearing in Dressler (1980) and the last column in each table give notes to each galaxy as indicated in the footnotes, showing which velocity values were used and other details. There is a faint chance of an occasional misidentification in the cluster A496, because our original finding chart was lost in the course of the reductions and a copy had to be used. We hope that no more than one galaxy may be misidentified, if at all. We point out the only significant velocity discrepancy in A496 is for galaxy No. 265 (a cD satellite) for which we quote a value 550 km s^{-1} lower than the previously published measurement.

We give in Table IV the external errors obtained for cluster galaxies comparing our data with data available in the literature, with references shown in Column 1, for the same galaxies as listed in Tables II and III. Column 2 gives the number of galaxies in common and Column 3 gives the mean of the velocity differences. On average, our velocities are shifted by 9 ± 38 km s^{-1}, with respect to the mean of all published cluster data (15 values).

Results of mean velocities and velocity dispersions for the clusters and their core regions (groups of faint galaxies around the central galaxies, defined and discussed in the next section) are given in Table V, where in Columns 3 and 4 we give redshifts and mean velocities corrected to the Local Group, using $V_0 = 300 \sin l^{\rm II} \cos b^{\rm II}$ km s^{-1} and including relativistic corrections; Columns 5 to 7 show the velocity dispersion with the corresponding 68% confidence limits calculated following the precepts of Danese *et al.* (1980) and the number of galaxies retained in the calculations having radial velocities within three standard deviations from the cluster mean velocity and survivors of a 3σ test which eliminates a galaxy with a velocity more than 3σ away from the mean velocity calculated without it (Yahil and Vidal 1977). Columns 8 to 11 show previous results for σ_v and their errors (68% confidence limits or standard deviations), number of galaxies used and references, with the same notation as in Tables II and III. Previous redshifts and mean velocities from the references are not quoted since those values are quite similar.

Dynamical masses of the clusters were calculated using mass estimators for self-gravitating systems of equal mass bodies from Heisler *et al.* (1985). These estimators are: virial mass MV, projected mass MP, average mass MA and median mass MM (assuming isotropic orbits), given by the formulas:

$$\mathrm{MV} = \frac{3\pi N}{2G}\frac{\Sigma_i v_{zi}^2}{\Sigma_{i<j} 1/R_{ij}},$$

$$\mathrm{MP} = \frac{f_{\mathrm{MP}}}{G(N-1.5)}\sum_i v_{zi}^2 R_i,$$

$$\mathrm{MA} = \frac{2f_{\mathrm{MA}}}{GN(N-1)}\sum_{i<j}(v_{zi}-v_{zj})^2 R_{ij},$$

$$\mathrm{MM} = \frac{f_{\mathrm{MM}}}{G}\mathrm{med}_{ij}\,[\,(v_{zi}-v_{zj})^2 R_{ij}\,],$$

where v_{zi} and distances R_i are relative to the galaxy centroid and $f_{\mathrm{MP}} = 32/\pi$, $f_{\mathrm{MA}} = 2.8$, and $f_{\mathrm{MM}} = 6.5$.

In the core region the virial mass was estimated assuming that the faint galaxies form a system of test particles orbiting

TABLE II. Velocities in cluster Sersic 40/6.

Gal. No. (1)	α(1950) (h m s) (2)	δ(1950) (° ′ ″) (3)	Lines[a] meas. (4)	cz (kms^{-1}) (5)	δ_v (kms^{-1}) (6)	cz (liter.) (kms^{-1}) (7)	δ_v (kms^{-1}) (8)	Ref.[b] (9)	Cross ident. (10)	Notes (11)
368	4 27 04.5	-61 25 30	7-8	17078	23					
844	4 27 15.2	-61 39 10	9	17184	27					
341	4 27 29.7	-61 24 46	7	16599	23					
679	4 28 01.7	-61 34 13	6	17588	34					
587	4 28 01.9	-61 31 38	11	17871	40					
732	4 28 31.0	-61 35 46	4	19398	37					
648	4 28 33.6	-61 32 59	8	17449	33					
217	4 28 37.7	-61 20 30				17900	110	MCTH82	01	i
240	4 28 37.8	-61 20 47				20000	110	MCTH82	02	i
620	4 28 44.8	-61 32 31	7-11	18437	32					
7173	4 28 47.6	-61 30 04	8	19095	30					
997	4 28 47.8	-61 47 12				19833	50	MQ81a	08	i
870	4 28 50.1	-61 40 57	7	19865	28					
253	4 28 51.7	-61 21 19				16862	300	MQ81a	09	
171	4 28 53.3	-61 18 56				19675	80	MQ81b	28	i
700	4 28 54.8	-61 34 31	9	18515	22					
121	4 28 58.3	-61 17 01				20000	50	MQ81b	27	i
1057	4 29 03.1	-61 49 17	7	17518	20					
916	4 29 04.7	-61 43 25	9	17697	26					
789	4 29 05.1	-61 37 21	5	16000	38					
547	4 29 13.2	-61 30 46	7	19118	31					
617	4 29 14.7	-61 32 49	5	17286	23					
812	4 29 35.1	-61 38 09	7	16586	30					
725	4 29 41.7	-61 35 12	7	19450	23					
822	4 29 42.5	-61 38 24				16630	100	MQ81a	04	i
						16681	134	GGP88	03	
						16869	144	WF80	03	
644	4 29 44.5	-61 33 24	7	18133	34					
783	4 29 47.1	-61 36 55	7	17148	27					
675	4 29 49.2	-61 34 21	5-5	18350	27					
697	4 29 59.2	-61 35 00	6	20124	34					
696	4 30 00.4	-61 34 43	6	18399	38					
500	4 30 01.6	-61 29 05				16600	140	MQ81a	05	i
672	4 30 02.0	-61 33 38	9	18956	27	18930	200	MQ81b	25	
524	4 30 05.2	-61 29 58	12	18769	21					
133	4 30 10.8	-61 17 58				13605	90	MQ81a	10	i
719	4 30 10.9	-61 35 34	10	18245	22					
694	4 30 12.8	-61 34 35	4	15303	34					
382	4 30 15.2	-61 26 35	9	16517	30					
671	4 30 17.0	-61 33 59	6	18687	53					s
820	4 30 17.3	-61 38 48	7-8	20150	20	20340	110	MCTH82	09	
819	4 30 17.4	-61 38 23				19600	130	MQ81b	11	i
						19703	79	GGP88	07	
						20210	110	MCTH82	10	
640	4 30 18.0	-61 32 58	4	18775	50					s
718	4 30 20.1	-61 35 20				17365	120	MQ81b	15	i
						17310	110	MCTH82	08	
865	4 30 20.6	-61 41 00				20340	80	MQ81b	20	i
717	4 30 22.4	-61 35 21	5	17428	53					
668	4 30 24.9	-61 33 46				16380	50	MQ81a	02	i-s
						16500	110	MCTH82	11	
752	4 30 26.6	-61 35 59	8	18729	33					
666	4 30 31.2	-61 33 56	7	18259	50					s
635	4 30 32.4	-61 33 02	10	17186	28					s
636	4 30 33.6	-61 33 32				18000	80	MQ81b	1E	i-db
						18052	25	CIEG85	–	
						18025	110	MCTH82	13	
						18270	84	WF80	02	
						18030		V75	01	

TABLE II. (continued)

Gal. No. (1)	α(1950) (h m s) (2)	δ(1950) (° ' ") (3)	Lines[a] meas. (4)	cz (kms^{-1}) (5)	δ_v (kms^{-1}) (6)	cz (liter.) (kms^{-1}) (7)	δ_v (kms^{-1}) (8)	Ref.[b] (9)	Cross ident. (10)	Notes (11)
663	4 30 32.4	-61 33 35				17705	50	MQ81b	1W	i-db
						17907	53	GGP88	04	
						17652	30	CIEG85	–	
						17780	110	MCTH82	12	
						17746	50	MQ81a	01	
						18020		V75	02	
897	4 30 34.6	-61 42 23				17740	70	MQ81b	21	i
612	4 30 36.2	-61 32 45	10	20573	31					
746	4 30 37.2	-61 36 26				15818	80	MQ81a	03	i
						15757	76	GGP88	02	
						15890	110	MCTH82	14	
						15777	87	WF80	01	
633	4 30 37.2	-61 32 51	6	15846	31					
539	4 30 39.5	-61 30 38				14445	145	MQ81b	12	i
						14258	62	GGP88	12	
1009	4 30 40.8	-61 47 24				17610	50	MQ81b	14	i
						17407	234	GGP88	16	
712	4 30 42.9	-61 35 26	6	16734	43					s
658	4 30 43.5	-61 33 46	3	17767	70					s
608	4 30 45.6	-61 32 15	6	19011	33					s
50	4 30 51.9	-61 13 28				17480	175	MQ81b	24	i
567	4 30 58.4	-61 31 35	12	17737	20	17660	200	MQ81b	26	
1023	4 30 59.9	-61 48 26	9	16222	29					
281	4 31 02.3	-61 23 29	6	21462	37					
535	4 31 07.2	-61 31 13	6	20508	51					
491	4 31 07.6	-61 29 4				14426	82	GGP88	13	i
601	4 31 09.0	-61 32 35				18845	60	MQ81b	23	i
775	4 31 10.9	-61 37 4	8	17581	36	17300	150	MQ81b	22	
709	4 31 15.1	-61 35 27	8	19530	25					
323	4 31 16.6	-61 24 45				17420	110	MQ81a	06	i
						17631	32	GGP88	08	
61	4 31 17.8	-61 14 17				17310	50	MQ81b	18	i
403	4 31 20.9	-61 26 51				18350	50	MQ81b	16	i
373	4 31 22.4	-61 26 3				16090	110	MQ81b	17	i
161	4 31 32.2	-61 18 48				18195	90	MQ81b	19	i
739	4 31 37.4	-61 36 07	7	18447	37					
159	4 31 44.0	-61 18 22				19505	50	MQ81b	13	i
482	4 31 45.2	-61 29 00	6	17002	28					
773	4 31 50.6	-61 36 59				16055	100	MQ81a	07	i
						16363	113	GGP88	09	
372	4 31 57.6	-61 26 12	9	17738	32					
593	4 32 0.5	-61 31 57	6-6	16878	58					
349	4 32 15.4	-61 25 23	7	16350	26					
590	4 32 18.3	-61 32 00	10	17653	20					
422	4 32 18.6	-61 27 50	7	21130	21					
203	4 32 27.2	-61 19 51	7	16133	40					
475	4 32 47.2	-61 29 05	9	17013	36					

[a] two values imply that two spectra were measured.

[b] References:
GGP88 : Green *et al.* (1988).
CIEG85 : Carter *et al.* (1985).
MCTH82 : Materne *et al.* (1982).
MQ81b : Melnick and Quintana (1981b).
MQ81a : Melnick and Quintana (1981a).
WF80 : West and Frandsen (1980).
V75 : Vidal (1975).

Notes :
(s) galaxy considered a satellite of central db.
(i) indicate values from literature used in all calculations in this paper.

TABLE III. Velocities in cluster A496.

Gal. No. (1)	α(1950) (h m s) (2)	δ(1950) (° ' ") (3)	Lines[a] meas. (4)	cz (kms^{-1}) (5)	δ_v (kms^{-1}) (6)	cz(liter.) (kms^{-1}) (7)	δ_v (kms^{-1}) (8)	Ref.[b] (9)	Cross ident. (10)	Dressler[c] number (11)	Notes (12)
32	4 28 43.7	-13 04 51	11	10519	33					-	IC0375
75	4 29 17.4	-13 15 21	6	30328	62					-	backgr.
83	4 29 21.8	-13 01 59				10336	100	PTSMC87	75	75	i
90	4 29 24.6	-12 47 19				9985	30	QMIT85	07	-	i
88	4 29 25.1	-12 51 57				10720	100	QMIT85	36	83	i
109	4 29 26.9	-13 28 49	7	9587	34					-	
103	4 29 38.3	-12 55 29	10	10020	28	10100	60	PTSMC87	78	78	
120	4 29 47.2	-13 11 21	4	9993	25					64	
135	4 29 56.9	-13 30 23				9120	80	QMIT85	29	34	i
						9107	60	PTSMC87	34		
126	4 30 04.3	-12 53 08				10700	30	QMIT85	20	82	i
145	4 30 08.1	-13 22 18				9640	70	QMIT85	25	51	i
143	4 30 10.2	-13 29 55				8305	30	QMIT85	28	33	i
						8301	60	PTSMC87	33		
146	4 30 12.4	-13 18 45				9000	30	QMIT85	10	60	i
147	4 30 17.2	-13 18 15				8800	100	QMIT85	24	59	i
						8937	100	PTSMC87	59		
164	4 30 25.6	-13 17 44	8	9815	50					58	
191	4 30 31.2	-13 00 54				10600	95	QMIT85	19	77	i
						10468	100	PTSMC87	77		
177	4 30 34.0	-13 28 51				9240	30	QMIT85	27	32	i
						9338	75	PTSMC87	32		
189	4 30 35.1	-13 05 10	6	8965	32					73	
180	4 30 35.6	-13 24 25	5	9419	51					40	
192	4 30 37.1	-12 52 58				10660	50	QMIT85	05	81	i
184	4 30 38.9	-13 18 35				9415	250	QMIT85	37	-	i
183	4 30 41.0	-13 22 17				10920	200	QMIT85	26	50	i
210	4 30 47.8	-13 42 13	10	10113	33					05	
205	4 30 50.0	-13 28 07	11	10334	35					31	
200	4 30 51.9	-13 10 11				9690	60	QMIT85	18	68	i
207	4 30 56.6	-13 34 06				9850	250	QMIT85	40	19	i
236	4 30 57.8	-13 15 21				9965	30	QMIT85	04	63	i
						9819	60	PTSMC87	63		
241	4 30 58.0	-13 05 16	6	10779	28					72	
226	4 30 59.0	-13 29 14	8	8320	20					30	
219	4 30 59.7	-13 37 03				9665	30	QMIT85	11	18	i
						9619	63	GGP88	07		
216	4 31 00.0	-13 39 14				9630	100	QMIT85	31	11	i
233	4 31 00.2	-13 22 51	13-15	11340	20					49	
235	4 31 02.4	-13 19 29	13	9349	30					48	
284	4 31 12.0	-13 29 01	8	10296	20	9950	250	QMIT85	35	39	
273	4 31 12.4	-13 23 09	4	9875	35					-	s
287	4 31 12.5	-13 31 36	7	9944	34					-	
261	4 31 12.9	-13 16 34	6	8868	20	9080	250	QMIT85	03	57	
283	4 31 15.0	-13 29 05	9	10368	25					28	
286	4 31 16.9	-13 31 47	10	8135	34					21	
253	4 31 17.0	-13 04 16	9	9206	33					74	
265	4 31 17.0	-13 20 57	9	9415	31	9960	100	HCW85	04	-	s
278	4 31 17.1	-13 20 24	9	9642	32					47	s
268	4 31 18.3	-13 21 34				9780	100	HCW85	03	-	i-s

TABLE III. (continued)

Gal. No. (1)	α(1950) (h m s) (2)	δ(1950) (° ′ ″) (3)	Lines[a] meas. (4)	cz (kms^{-1}) (5)	δ_v (kms^{-1}) (6)	cz(liter.) (kms^{-1}) (7)	δ_v (kms^{-1}) (8)	Ref.[b] (9)	Cross ident. (10)	Dressler[c] number (11)	Notes (12)
263	4 31 18.5	-13 21 15	6	9984	32					-	s
270	4 31 18.7	-13 21 56	5	9868	30	9863	30	Q89	-	46	im-cD
						9743	37	GGP88	01		
						9705	60	PTSMC87	46		
						9876	16	T85	-		
						9760	30	QMIT85	01		
						9840	100	HCW85	01		
258	4 31 19.4	-13 09 27	4-7	9718	24					66	
271	4 31 19.6	-13 22 03				9870	100	HCW85	02	-	i-s
						9814	21	T85	-	-	
272	4 31 20.5	-13 22 26	8	9799	33					-	s
281	4 31 20.6	-13 26 47	8	9973	40					27	
277	4 31 21.9	-13 24 16	10	9651	39					38	s
262	4 31 22.4	-13 16 27				9830	250	QMIT85	02	56	i
						9851	60	PTSMC87	56		
300	4 31 23.8	-13 26 38				10200	50	QMIT85	34	26	i-s
						10290	75	PTSMC87	26		
318	4 31 25.5	-13 05 54	9	9427	24					-	
306	4 31 29.8	-13 18 40	7	9856	20					-	s
305	4 31 32.3	-13 21 08				11025	60	QMIT85	33	45	i
342	4 31 38.2	-13 33 58				9510	50	QMIT85	13	15	i
						9733	124	GGP88	08		
337	4 31 43.0	-13 24 00	6	9185	52					37	
341	4 31 45.0	-13 34 01				8535	100	QMIT85	30	14	i
335	4 31 48.2	-13 21 28	6	9513	47					44	
358	4 31 50.8	-13 20 47	7	10101	38					43	
356	4 31 51.5	-13 28 24				10525	100	QMIT85	14	25	i
						10489	100	PTSMC87	25		
362	4 32 00.1	-12 54 10	8	9863	49					-	
405	4 32 16.8	-13 27 30	7	10191	29					24	
407	4 32 27.9	-13 35 15				9925	35	QMIT85	15	13	i
						9983	60	PTSMC87	13		
408	4 32 29.5	-13 40 11	5	10596	47					08	
403	4 32 36.6	-13 17 36				9560	30	QMIT85	39	55	i
431	4 32 43.6	-13 00 00				9535	120	QMIT85	22	76	i
418	4 32 46.8	-13 34 22	7	9810	36					12	
421	4 32 48.1	-13 29 48	6	9391	41					23	
422	4 32 49.7	-13 24 45				10405	100	QMIT85	32	35	i
425	4 32 51.9	-13 20 47				10555	90	QMIT85	16	42	i
						10462	60	PTSMC87	42		

[a] two values imply that two spectra were measured.

[b] References:

Q89 : Quintana unpublished (1989):
LCO Dupont telescope, 2DF observations.
GGP88 : Green *et al.* (1988).
PTSMC87: Proust *et al.* (1987).
QMIT85 : Quintana *et al.* (1985).
T85 : Tonry (1985).
HCW85 : Hu *et al.* (1985).

[c] Dressler (1980).

Notes :

(s) galaxy considered a satellite of central cD.
(i) indicate values from literature used in all calculations in this paper.
(im) indicate that the mean of all values listed was used in calculations: 9808 $\pm$ 30 kms^{-1}

TABLE IV. Comparison of velocities

Reference	Number of galaxies	Δv^a $\mathrm{km s^{-1}}$
(1)	(2)	(3)
MQ81b	(3)	128±110
MCTH82	(1)	-190±112
QMIT85	(3)	81±280
HCW85	(2)	-259±326
T85	(1)	-8± 34
PTSM87	(3)	42±171
GGP88	(1)	125± 48
Q89	(1)	5± 36
Total	(15)	9± 38

[a] Error is the standard deviation of the unweighted mean of individual differences.

around a massive object (Bachall and Tremaine 1981), calculating virial mass

$$\mathrm{MV} = \frac{3\pi}{2G} \frac{\Sigma_i v_{zi}^2}{\Sigma_i 1/R_i}$$

and projected mass

$$\mathrm{MP} = \frac{16}{\pi G N} \sum_i v_{zi}^2 R_i,$$

where v_{zi} and R_i are relative to the central galaxy. Therefore, in this calculation we left out the central galaxy velocity. The errors for the Heisler *et al.* estimators were determined from the variance of results of large number of cluster simulations [more than 10 000 clusters of 20, 80, and 320 galaxies, fitted by a King (1966) model] where those estimators were used to calculate the known mass in each model with different number of galaxies and assumed velocity dispersions. The simulation results show that all estimators are very stable and have excellent correlation between them, as shown when applied to groups by Heisler *et al.* For the core mass calculations, the uncertainties are variances obtained from simulations done for groups with 5–20 members. Masses are given in Table VI, where Column 3 shows the number of galaxies retained in each of the determinations and Columns 4, 5, 6, and 7 show MV, MP, MA, and MM, in unit of $10^{14} \mathscr{M}_\odot$.

To complement the velocity analysis, we constructed isopleths from galaxy counts extending well out into the cluster neighborhood. An area of 5°×5° around A496 was inspected on a 90 min baked IIIa-J plate taken under good seeing (∼l'') with the Curtiss–Schmidt telescope at Cerro Tololo Inter-American Observatory in January 1989. A total of 1582 galaxies were counted with positions measured, approximately down to 18 mag. Counts were performed on the J ESO/SRC survey field 118 (film copy) around Sersic 40/6. Here 1395 galaxies were measured, down to 18 mag (the number was higher for fainter magnitudes, but completedness was reached at the magnitude quoted), again in an area 5°×5° centered on the cluster.

Number density maps and isopleth contours are shown in Figs. 1 and 2, where the ordinate is the number density of galaxies. Also shown are density maps of the central regions, obtained in similar fashions, from the counts restricted to an area of 1.2°×1.2° for A496 and from unpublished data covering a 40′×40′ field obtained from a prime-focus CTIO 4 m telescope IIIa-J plate for Sersic 40/6. Densities were calculated in a grid of 100×100 points, using the nearest 10 or 12

TABLE V. Cluster mean velocities and velocity dispersions.

Cluster name	Sample	z	v ($\mathrm{kms^{-1}}$)	σ_v ($\mathrm{kms^{-1}}$)	error ($\mathrm{kms^{-1}}$)	N	σ_v(liter.) ($\mathrm{kms^{-1}}$)	error ($\mathrm{kms^{-1}}$)	N	Ref.
(1)	(2)	(3)	(4)	(5)	(6)	(7)	(8)	(9)	(10)	(11)
Ser40/6	cluster	0.0588	17359 ± 167	1440	(+126 , -110)	84				
							1410		29	CTG84
							1517	(+252 , -167)	29	MQ81b
							1836	± 581	16	MCTH82
							1461	(+479 , -243)	11	MQ81a
Ser40/6	core		17432 ± 219	684	(+208 , -109)	12				
A496	cluster	0.0319	9649 ± 78	619	(+61 , -47)	70				
							657	(+104 , -72)	32	QMIT85
A496	core		9647 ± 65	188	(+63 , -34)	11				

References :
MQ81a : Melnick and Quintana (1981a).
MQ81b : Melnick and Quintana (1981b).
MCTH82 : Materne *et al.* (1982).
QMIT85 : Quintana *et al.* (1985).
CTG84 : Carter *et al.* (1984).

TABLE VI. Cluster and core dynamical masses.

Cluster (1)	Sample (2)	N (3)	MV 10^{14} $M_\odot$ (4)	MP 10^{14} $M_\odot$ (5)	MA 10^{14} $M_\odot$ (6)	MM 10^{14} $M_\odot$ (7)	Notes (8)
Ser40/6	cluster	84	34.8 ± 6.0	48.0 ± 9.0	38.3 ± 7.0	30.8 ± 7.0	a
	core	12	1.4 ± 1.1	2.3 ± 1.5	1.5 ± 1.0	1.6 ± 0.7	a
		10	0.7 ± 0.1	1.2 ± 0.5			b
A496	cluster	70	5.6 ± 1.0	7.8 ± 1.0	6.2 ± 1.0	5.3 ± 0.4	a
	core	11	0.061±0.050	0.138±0.090	0.094±0.070	0.048±0.030	a
		8	0.029±0.019	0.041±0.020	0.026±0.018	0.020±0.011	a
		10	0.018±0.003	0.066±0.026			b
		7	0.011±0.002	0.021±0.010			b

[a] Based on equal mass bodies calculations, assumes isotropic orbits (Heisler *et al.* 1985).
[b] Based on test particles orbiting a massive object (db or cD), assumes isotropic orbits (Bahcall and Tremaine, 1981).

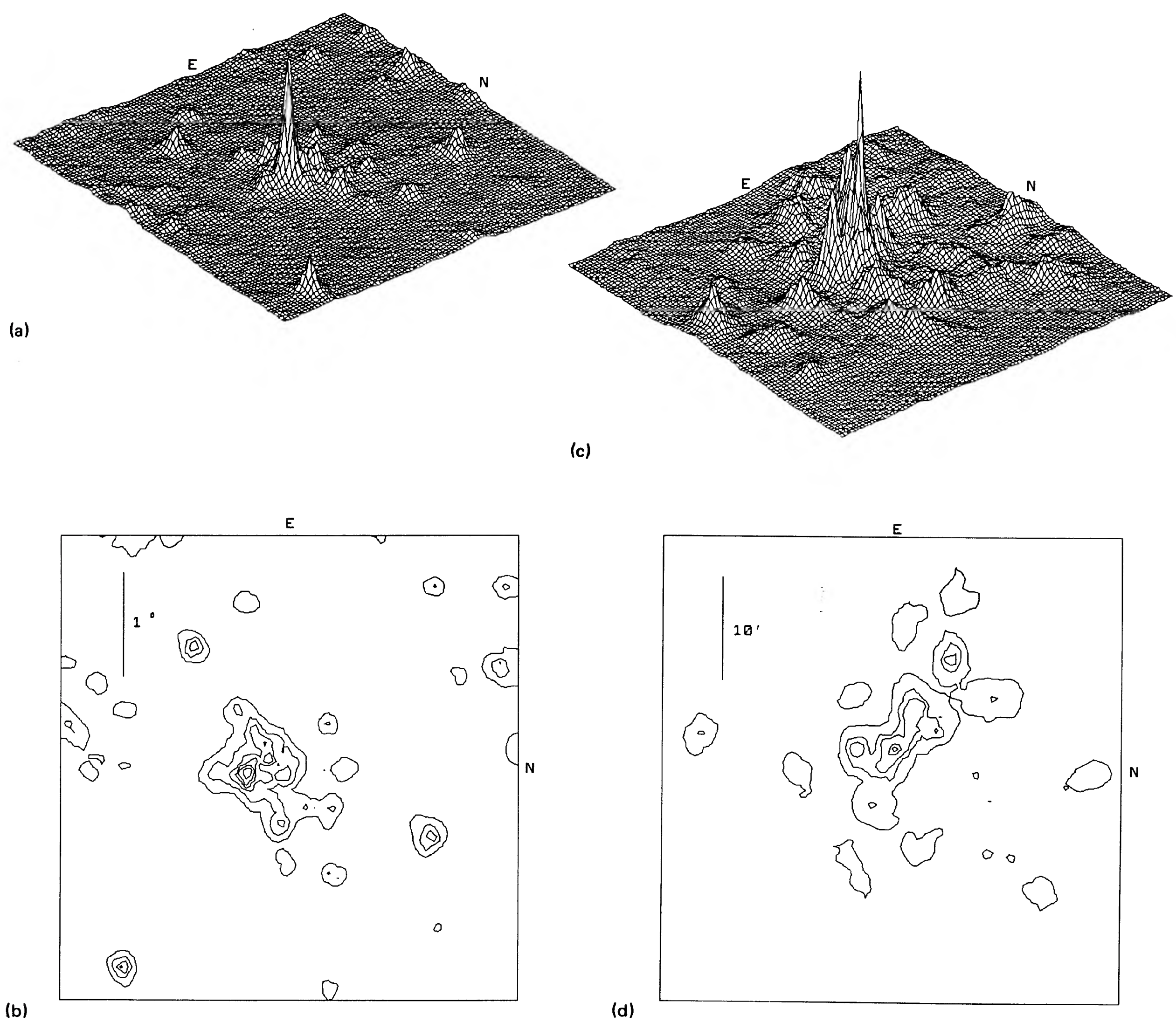

FIG. 1. (a) and (b): Surface and contour maps of Sersic 40/6 in a total area of 5°×5° from counts down to approximately 18 mag galaxies. The contours are at levels of 0.06, 0.12, 0.20, 0.32, 0.50, 0.80 gal/arcmin^2. (c) and (d): Surface and contour maps of Sersic 40/6 in an central area of 40′×40′ from counts down to approximately 21 mag galaxies. The contours are at levels of 1, 2, 3, 6, 8 gal/arcmin^2.

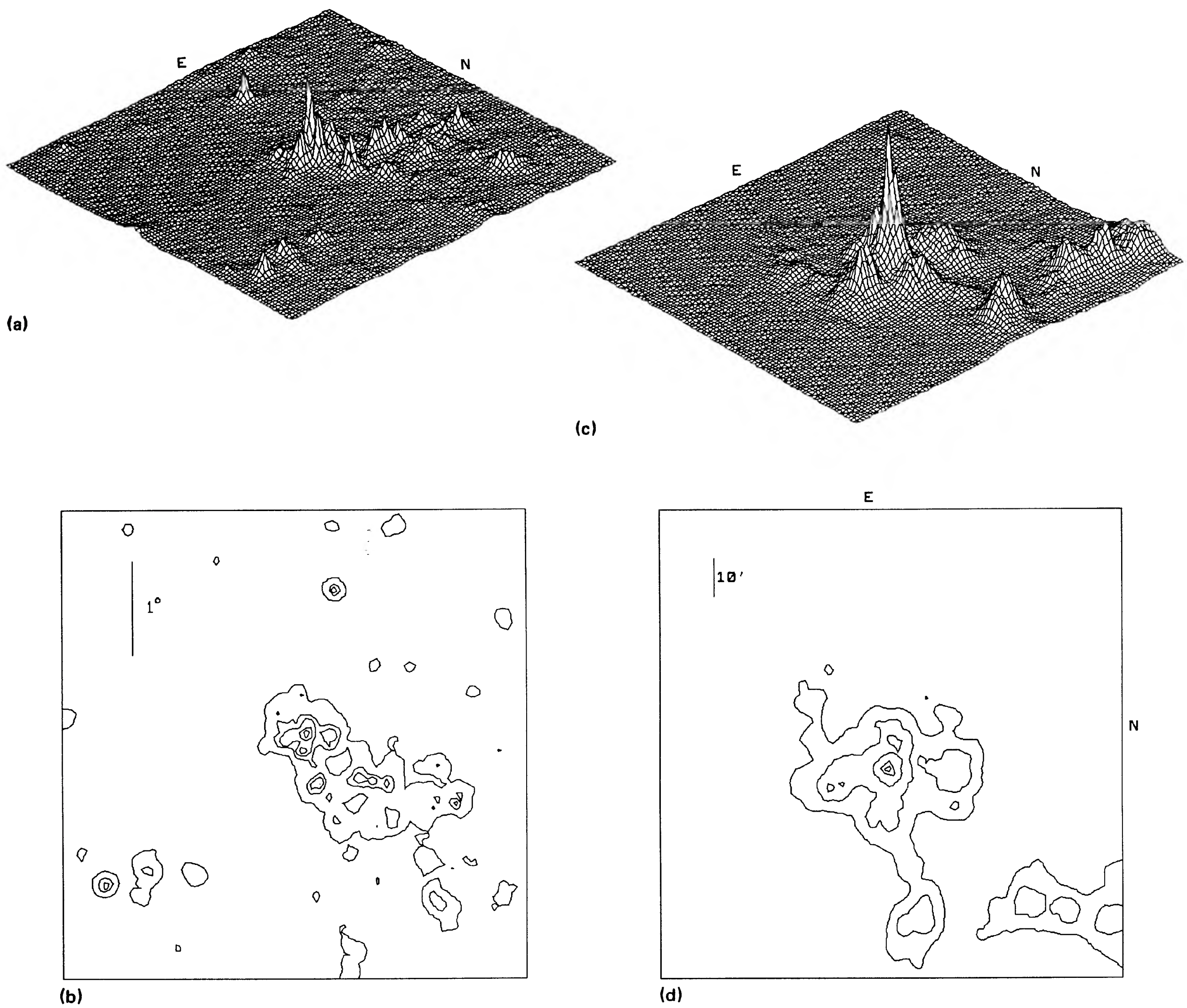

FIG. 2. (a) and (b): Surface and contour maps of A496 in a total area of 5°×5° from counts down to approximately 18 mag galaxies. The contours are at levels of 0.08, 0.20, 0.32, 0.55, 0.90 gal/arcmin^2. (c) and (d): Surface and contour maps of A496 in an central area of 1.2°×1.2° from the same counts. The contours are at levels of 0.15, 0.32, 0.64, 1.20, 1.60 gal/arcmin^2.

members (10 for A496 and 12 for Sersic 40/6) divided by the area of the circle containing them. This density determination method affords to keep reasonable statistics per bin (pixel) providing at the same time high resolution at the cluster centers.

IV. DISCUSSION

a) Sersic 40/6

This is a rich cluster with coordinates R.A. (1950): $04^h 30^m 30^s$ and Dec. (1950): $-61°35'$, as listed in the new Abell *et al.* (1989) catalog; optically, it is centered in a db galaxy (offset 98 arcsec from above position) which has been spectroscopically studied by Carter *et al.* (1985). The cluster is a strong x-ray source with a luminosity of $L_x = 10^{44.54}$ ergs^{-1} in the 2–6 keV band (Kowalski *et al.* 1984) and is associated to the 2A0431-61 (Ariel V, Cooke *et al.* 1978), 4U0427-61 (Fourth *Uhuru* catalog, Forman *et al.* 1978) and 1H0429-616 (HEAO A-1, Wood *et al.* 1984) x-ray sources.

The density surfaces and contours of Figs. 1(a)—1(d) in the 5°×5° and central 40′×40′ areas, down to 18 and 21 mag, respectively, show a regular global structure with the presence of some small-scale enhancements which, however, cannot be associated to any specific velocity subgroups in our data. There is a secondary density spike some 12′ at direction NE from the center, mainly formed by faint galaxies.

The velocity histogram of 84 galaxies shown in Fig. 3(a) has a Gaussian profile distribution centered at a heliocentric velocity of 17 815 km s^{-1} ($\sim$17 360 km s^{-1} with relativistic correction), slightly asymmetric with an extended tail to high velocities. The Gaussian fit of all galaxies, excluding the dumbbell galaxy, gives an average with a difference of 38 km s^{-1} from the db mean velocity, implying an 81% of probability that the distribution is centered at the db mean

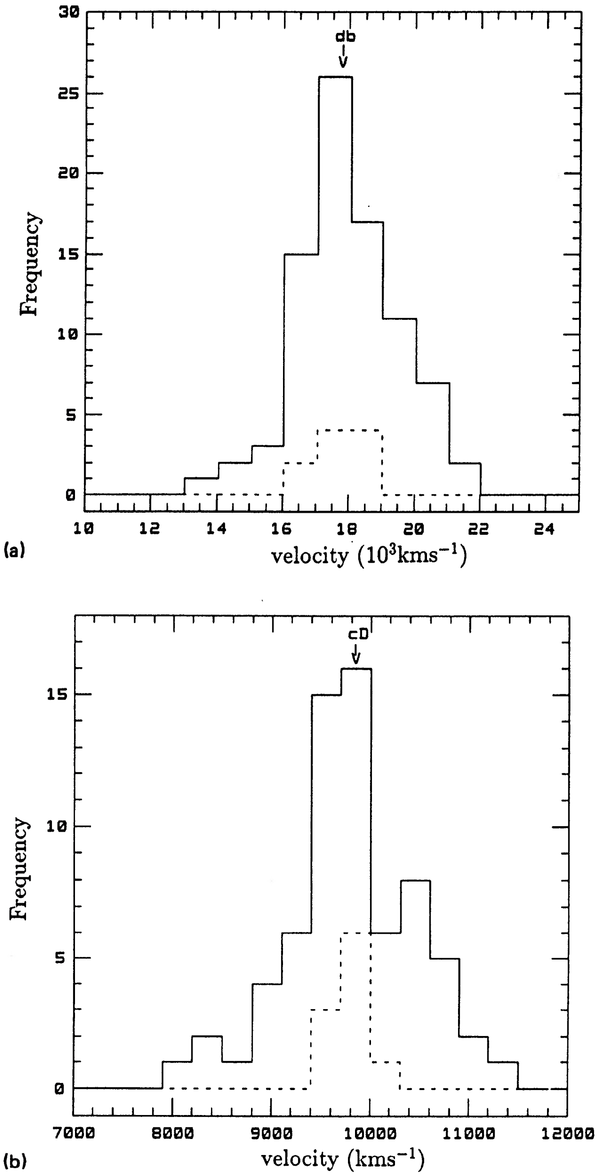

FIG. 3. (a) Histogram of velocity of 84 galaxies of Sersic 40/6. Each bin is 500 km s^{-1} wide. (b) Histogram of velocity of 70 galaxies of A496. Each bin is 300 km s^{-1} wide. The arrows show the cD or db mean velocities and the dashed lines the histograms of the core bound regions.

velocity (Quintana and Lawrie 1982). For the db itself we have used the data from Melnick and Quintana (1981b), which gives the same db mean that the high-quality spectrum from Carter *et al.* (1985), though their velocities give a relative difference between db components of 400 km s^{-1} instead of 300 km s^{-1}. Melnick and Quintana (1981b) noted the high velocity dispersion σ_v of this cluster, first determined from only 11 galaxies, in poor agreement with the L_x–σ_v relation (Quintana and Melnick 1982). The present work gives a slightly lower value of σ_v with a much reduced uncertainty, but still in poor agreement with that relation. This high velocity dispersion could have been explained perhaps by the presence of groups seen in projection. We have analyzed the velocity histograms determined in concentric rings, as shown in Fig. 4(a). As seen in the figure the dumbbell mean velocity is near the mean velocity in all rings. The histograms are slightly flatter in the middle rings but narrow in the two outer ones. The outermost ring is shifted from the cluster mean but it has very low statistical value with only three galaxies. In Fig. 5(a) we show the variation of the velocity dispersion as a cumulative function of the number of galaxies, counted from the center, and in Fig. 5(b) we show its variation in concentric rings, which have been chosen with approximately 12 galaxies each, to compare results with similar statistical uncertainties. As it can be seen in Fig. 5(b), the dispersion values fluctuate within statistical uncertainties and are consistent with a constant σ_v, except near the center. This analysis does not identify projected groups in the cluster by significant distortions in the histogram or velocity dispersion profiles. However, in view of the reduced number of 84 velocities available, one should not discard completely the existence of outlying groups.

If we consider the central galaxies: the dumbbell and its eight closest neighbors, we find that the velocity dispersion of this group is significantly lower than the overall cluster value, as shown in Figs. 5(a) and 5(b). Materne *et al.* (1982) analyzed the number density profile and fitted the radial distribution with a two-component model because the isothermal model fit was not good in the core region, i.e., inside 4 arcmin from the cluster center. This is approximately the same region containing the galaxies showing the low velocity dispersion value. Figure 6(a) shows the density profile obtained from our counts, where the spike within 0.18 Mpc is apparent, corresponding to $\sim 2'$ from the db. Together with the density results from Materne *et al.* (1982), this finding permits us to suggest that a subsystem dynamically bound is present at the center of this cluster, a dynamical cusp. The dumbbell mean velocity of 17 853 km s^{-1} has a 99% of probability to be coincident with the core mean velocity in view of their difference of 2 km s^{-1}, obtained from a Gaussian fit to the velocity histogram of the other eight core galaxies (Nos. 570, 635, 640, 658, 666, 668, 671, and 712). Carter *et al.* (1985) showed that the velocity dispersion of this db system grew from approximately 250 km s^{-1} at the nuclei, to approximately 600 km s^{-1} in the halo at 25″–30″ from the brighter nucleus. Thus, this dispersion agrees well with the dispersion of 700 km s^{-1} of the cusp galaxies (ten in total). This fact strengthens the hypothesis that the central group forms a bound system with the db.

Tables V and VI show the mean velocity, velocity dispersion, and dynamical mass of the cluster and core subsystem, if assumed bound. The cluster mass ranges between $(2.9 \pm 0.7) \times 10^{15}\ \mathcal{M}_\odot$ and $(4.7 \pm 0.9) \times 10^{15}\ \mathcal{M}_\odot$, with only the projected mass much higher than the other estimators. We can take as a representative value the virial mass determination, at approximately $(3.0 \pm 1.0) \times 10^{15}\ \mathcal{M}_\odot$. There are also differences between the mass values obtained for the core subsystem, but they are all consistent within the rather high estimated errors. All numbers for mass determination indicate that the db mass, of approximately $(2.1 \pm 1) \times 10^{14}\ \mathcal{M}_\odot$, is at the very top of cD galaxy masses. The key question is whether the dumbbell galaxy and its surrounding group really forms a relaxed bound system, as the evidence presented suggests.

It will be interesting to investigate with numerical models the influence that the tidal effects of the group have in heating up the dumbbell halo and, conversely, to see if the binary

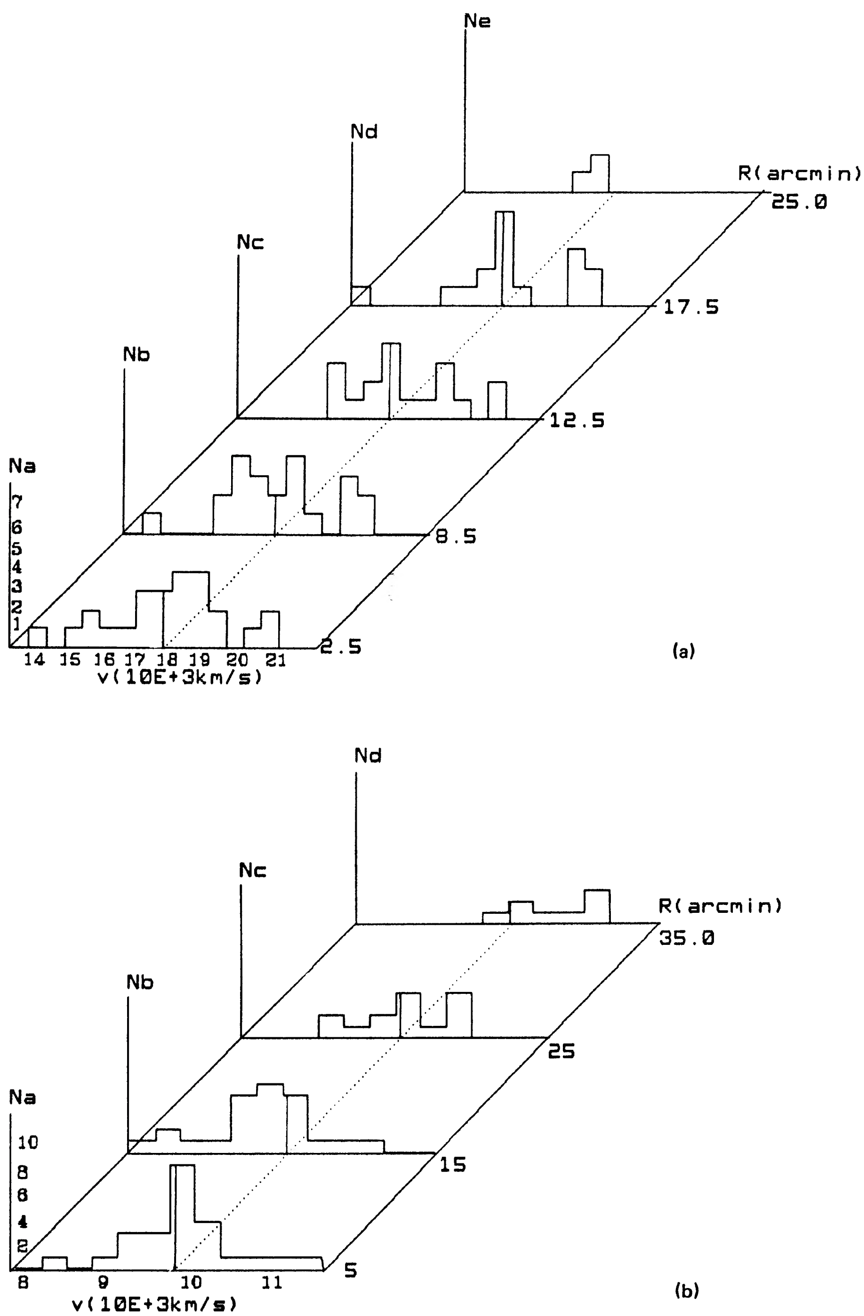

FIG. 4. (a) Histograms of velocity in concentric rings at different radii from the center of the cluster Sersic 40/6. The number of galaxies in each ring are: Na = 25, Nb = 22, Nc = 18, Nd = 16, Ne = 3. Bin size is 500 km s^{-1} wide. (b) Histograms of velocity defined in similar manner for A496. The number of galaxies in each ring are: Na = 25, Nb = 23, Nc = 14, Nd = 8 and the bin is 300 km s^{-1} wide. The dotted lines show the cD or db mean velocities.

galaxy transfers energy to the core members, offsetting infall due to dynamical friction. Alternatively, the db halo could have been partly due to the tidal debris of the group galaxies infalling to the central position. This halo would maintain the group dispersion. Analysis considering the dumbbell system rotation or the merging parameters of the group are necessary to clarify these matters, as the halo shows typical distortions seen in other double elliptical dumbbell systems.

b) A496

This is a rich cluster centered in a cD galaxy. It has an x-ray luminosity $L_x = 10^{43.83}$ ergs^{-1} in the 2–6 keV band (Kowalski *et al.* 1984) and is associated to the 2A0431-136 (Ariel V, Cooke *et al.* 1978), 4U0431-12 (Fourth *Uhuru* catalog, Forman *et al.* 1978) and 1H0430-133 (HEAO A-1, Wood *et al.* 1984) x-ray sources. This cluster has been studied in detail because of its strong central cooling flow. Fabian *et al.* (1981) reported the discovery of an optical filamentary system around the central galaxy, but Cowie *et al.* (1983) and Hu *et al.* (1985) did not find it. From the x-ray emission a flux of $\sim 200\,\mathcal{M}_\odot$ yr^{-1} infalling to the cD was estimated by Nulsen *et al.* (1982), assuming a velocity dispersion of 800 km s^{-1}, which is closer to $300\,\mathcal{M}_\odot$ yr^{-1} using Quintana *et al.* (1985) result of $\sigma = 650$ km s^{-1}, with similar values from the present work. Hu *et al.* (1985) made long-slit spectroscopy of the gas in the cD detecting nuclear emis-

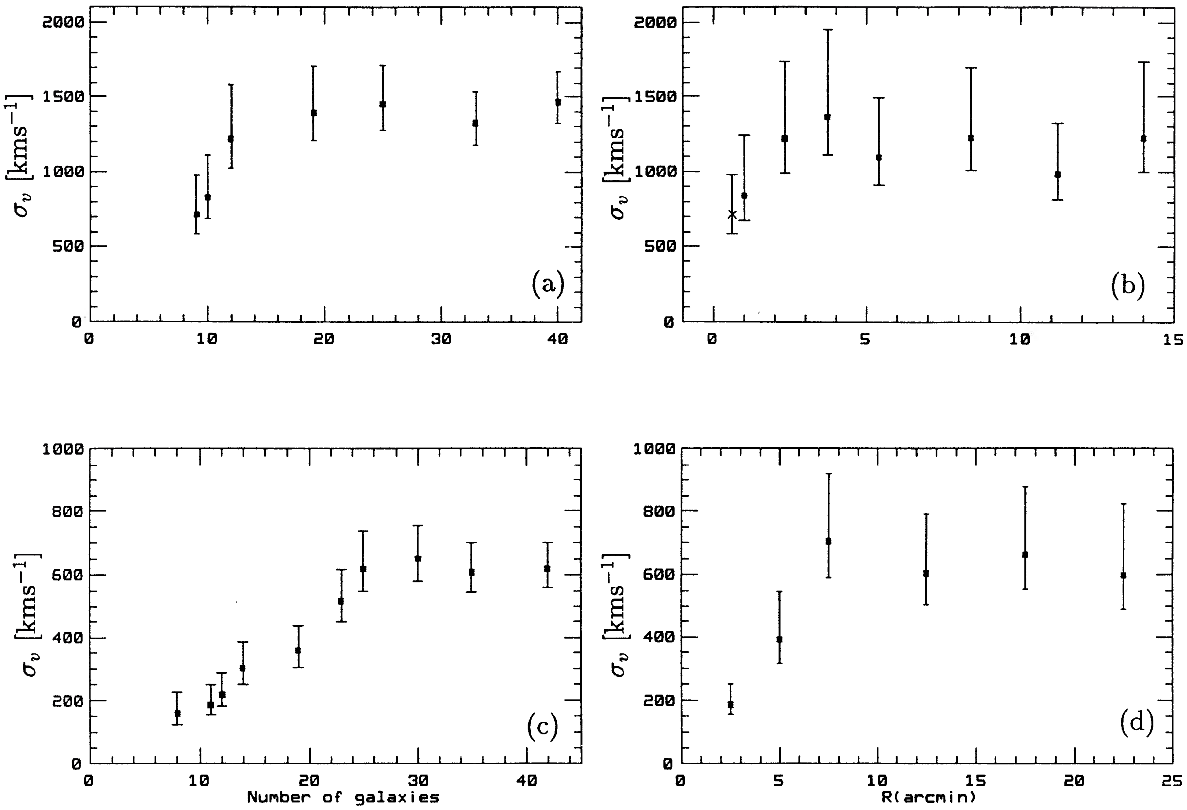

FIG. 5. Plots of the velocity dispersions in the clusters. In Sersic 40/6: (a) as a cumulative function of the number of galaxies from centered db. (b) differential values as a function of radius in rings having 12 galaxies; the symbol × shows the core velocity dispersion. In A496: (c) as a cumulative function of the number of galaxies from centered cD. (d) differential values as a function of radius in rings having 16 galaxies. Error bars are 68% confidence limits.

sion and showing that it was extended, symmetrically distributed at the nucleus and stretching slightly less than $\pm$ 10 arcsec. In a region of approximately 8×8 arcsec the Hα, [N II] complex has a velocity dispersion higher than 1000 km s^{-1} with an asymmetric profile, likely due to the infalling velocity.

In our counts of galaxies in a 5°×5° area shown in Figs. 2(a) and 2(b) a clear asymmetric global structure appears, with the northwest quadrant having a higher density which produces a large elongation in the cluster shape. Because there are two nebulae in the southeast quadrant (LBN 0981: bright nebula and LDN 1642: dark nebula) the counts of faint galaxies are likely not complete in that area and bright galaxies appear obscured. It is difficult to know if the apparent density enhancement in the northwest quadrant could only be due to obscuration in other quadrants. Close to the cluster main body, i.e., within 1.2°×1.2°—the distribution of bright galaxies (13 to 17 mag) also shows a substructure at northwest [see Figs. 2(c) and 2(d)]. Velocities of galaxies there give a mean value of 10 420 $\pm$ 291 km s^{-1} with a dispersion of 298 (+ 144, − 62) km s^{-1}. Almost all of them are included in the northwest group of galaxies, noted A, in Mazure *et al.* (1986). Other smaller substructures are weakly apparent but they have high velocity dispersions. There are three dense regions around the central group, as shown in Fig. 2(c). However, none of them coincides with the elongated south–north structure reported by Mazure *et al.* (1986). The center of the global structure is offseted to east from the central cD galaxy when bright magnitudes only are included in the density calculations.

This cluster shows a group of satellites to the cD which forms a density spike or cusp, as is apparent in Figs. 2(a) and 2(c). The density profile is shown in Fig. 6(b) where the density cusp is visible within the inner 0.2–0.3 Mpc.

The velocity histogram of the whole cluster has a Gaussian profile [see Fig. 3(b)]. The distribution of galaxies in different outgoing rings show flatter histograms, except at the center, as is shown in Fig. 4(b). The velocity histogram of the second ring, including galaxies from 10′ to 20′ in radius, has a significant asymmetry produced by a group of galaxies (including Nos. 253, 318, 258, 200, 164, 184, 147, 146, 145, 180, 177, 143, 207, 219, 216, 342, and 341), most of them west from the cD and belonging to a region with high density. As in Sersic 40/6, the velocity histogram narrows in the two outer rings, indicating a lack of high relative velocity galaxies in the outer parts as expected for radial or circular orbits. The outermost ring has some galaxies at high relative velocity from the cD that also causes a slight asymmetry in the overall velocity histogram as discussed (group A). Figures 5(c)–5(d) show the velocity dispersion versus distance as a function of the number of galaxies from the center and as a function of radius in different rings with similar number of galaxies. The velocity dispersion in the central regions decreases continuously as the cD is approached. Within the

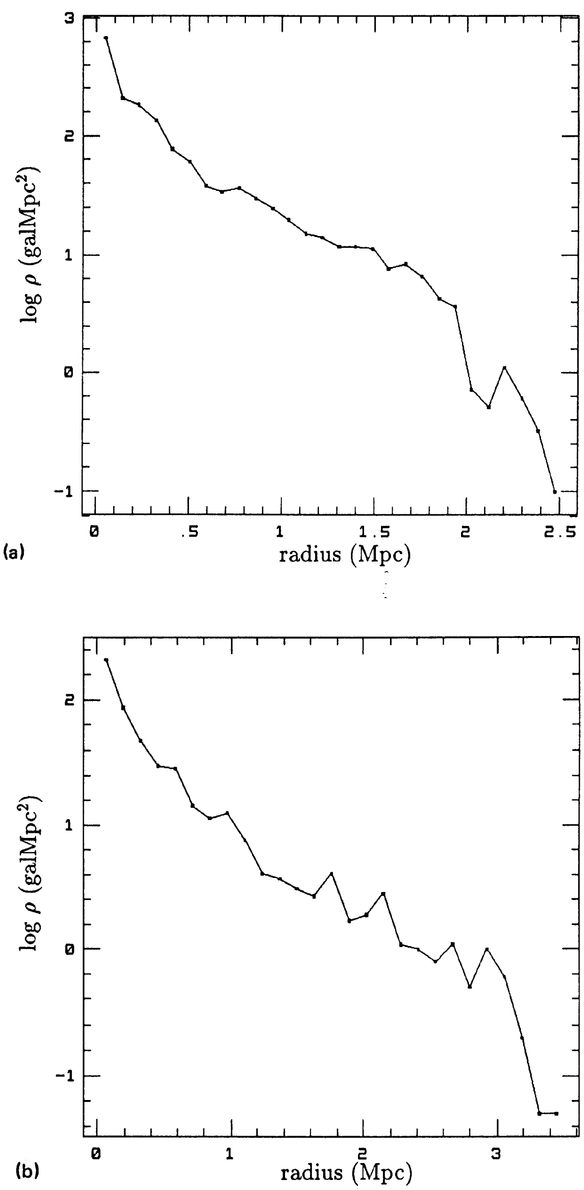

FIG. 6. (a) Density profile of Sersic 40/6 from counts of a sample of 1007 galaxies down to 21 mag. (b) Density profile of A496 from counts of a sample of 355 galaxies, down to 18 mag, approximately.

internal 5 arcmin the velocity dispersion of 14 galaxies is 303(+ 85, − 50) km s^{-1} and increases to 671(+ 112, − 75) km s^{-1} for galaxies within 10 arcmin, decreasing slightly outwards. Moreover, as shown in Table V, a dispersion of 188 (+ 63, − 34) km s^{-1} is obtained for the inner 4′ where 11 members are considered (Nos. 263, 265, 268, 270, 271, 272, 273, 277, 278, 300, and 306), leaving out two galaxies (Nos. 233 and 305) whose velocities are far away from the core mean value and are rejected by the $3\sigma_v$ test applied to this group. This core has a 99% of probability that the cD's velocity coincides with the center of the histogram Gaussian fit because of a 1 km s^{-1} velocity difference (Quintana and Lawrie 1982). There is also a 99% of probability of coincidence when all cluster galaxy velocities are considered. Moreover, if we take just the inner eight galaxies, within 2′, one obtains a dispersion of ~160 km s^{-1}. We can then safely assume that the inner ten galaxies are bound to the cD. In effect, the internal dispersion of the cD is 275 ± 12 km s^{-1} (Tonry 1985), which is comparable to the core dispersion of 188 km s^{-1}.

The dynamical mass of the cluster and core, the later calculated under the two assumptions that the closest 7, or 10, galaxies are bound to the cD, are given in Table VI. We obtain cluster masses between 5.4–7.5(± 1) $10^{14}\,\mathcal{M}_\odot$, approximately, and core masses in the range $(2.1 \pm 1.0)\times 10^{12}\,\mathcal{M}_\odot$ to $(15.6 \pm 1.0)\times 10^{12}\,\mathcal{M}_\odot$, depending on the method applied and taking seven or ten galaxies. A representative value for the core mass can be taken as $(7.0 \pm 2.0)\times 10^{12}\,\mathcal{M}_\odot$, while a similar value for the cD mass is $(2.5 \pm 1)\times 10^{12}\,\mathcal{M}_\odot$ (from the inner 8 galaxy core). If we take this $2.5\times 10^{12}\,\mathcal{M}_\odot$ cD mass the large cooling flow in this cluster (200–300 $\mathcal{M}_\odot$ yr^{-1}) operating over 10^{10} yr, could have produced the cD, if formed by deposition of cooling flow mass.

c) Dynamical Evolution

At present there is no concensus on the governing factors and rates of evolution in clusters, particularly concerning the cannibalism hypothesis. The subject has been recently reviewed by Merritt (1988).

The core of A496, with a velocity dispersion below 200 km s^{-1}, is in all likelihood bound to the cD. Using numerical simulations, Merrit (1983, 1985), has shown that tidal truncation of galaxy halos by the cluster field implies that little dynamical evolution could be expected after virialization, the importance of the effect depending on the amount of matter in dark form. Truncation will lower galaxy sizes essentially to the values of the visible galaxy (radius less than 30 kpc), resulting in dynamical friction effects drastically reduced. Typical timescales for orbits decay become comparable to a Hubble time. Merrit also showed that orbits decay with constant shape, so most of the orbits will have very significant ellipticities if initial orbits were mostly the product of the formation collapse. Galaxies in these orbits are the candidates for cannibalism.

When galaxies loose mass and approach the cluster core, the phenomena of equipartition, lighter galaxies acquiring kinetic energy from more massive ones and moving to outer orbits, will tend to counteract dynamical friction effects. In this view, very few galaxies will be cannibalized by the central cD. However, if a faint galaxy gets within the denser halo of the cD, the calculations of Zavitsky and White (1988), Hernquist and Weinberg (1989), and Bontekoe and van Albada (1987) show that merging times are of order 10^9 yr, for a 1/10 mass ratio between the cannibal and the satellite. However, as Hernquist and Weinbert (1989) point out, important issues remain in understanding the orbit decay, though it seems the latest numerical simulations are providing consistent results.

The picture advocated by Merritt (1985) is that cD's are formed early in the life of the cluster with little subsequent growth due to capture and mergers of other cluster member galaxies. The amount of capture rate will depend strongly on the cluster velocity dispersion. In clusters with dispersions of 500 km s^{-1} or lower, it can be expected that up to one L_* (Schechter 1976) is accreted in 5×10^9 yr. The same effect is expected if more than 20% of the cluster mass is attached to galaxies. But very little evolution can be expected in a cluster with a dispersion of 1500 km s^{-1}, like Sersic 40/6.

In this paper we have presented data on two clusters that fall on extremes of velocity dispersions. Bothun and Schombert (1988) looked at central velocities in three cD clusters and in only one, A2589, found a density cusp with a central velocity dispersion of 170 km s^{-1}, comparable to the cusp's dispersion in A496. Such low central dispersion in A496 argues in favor of a bound cusp of galaxies. Most of the galaxies in this cusp have low luminosities, and consequently, low masses (any dark halos should have long been stripped). The global dispersions are also comparable in A496 and A2589, so the rates calculated by Bothun and Schombert (1988) are applicable to A496.

Following Binney and Tremaine (1988) or Bothun and Schombert (1988), the general formula for the dynamical friction time for a galaxy of mass $\mathscr{M}$ and luminosity L moving in radial orbit in the cD halo is given, in astrophysical units, by

$$T_{\rm df} = \frac{5\times 10^{10}\ {\rm yr}}{\ln \Lambda}\left(\frac{R}{300\ {\rm kpc}}\right)^2\left(\frac{V_{\rm rel}}{1000\ {\rm km\ s^{-1}}}\right) \times\left(\frac{\mathscr{M}/L}{10}\right)^{-1}\left(\frac{L}{10^{11}L_\odot}\right)^{-1},$$

where R and $V_{\rm rel}$ are the typical distance and relative velocity of the companion galaxy relative to the cD center. The factor $\ln \Lambda$ is related to the maximum impact parameter, $b_{\rm max}$. Following Bothun and Schombert (1988), we also take $\ln \Lambda = 4.2$ for the reasons given there. In A496 we have $R \simeq 100$ kpc, $V_{\rm rel} \simeq \sqrt{3}\times 190$ km s^{-1}, $L \simeq 5\times 10^9\ L_\odot$ for faint companion galaxies and we can conservatively take $\mathscr{M}/L = 10$, with $b_{\rm max} \sim 1$ Mpc (cD halo sizes). These values give for A496, $T_{\rm df} \simeq 7\times 10^9$ yr. This time is long enough that there is a chance of seeing galaxies in this phase, but is short enough to represent an evolution in the cluster timescale. However, for Sersic 40/6 the application of the formula with similar parameters for companion masses, luminosities and radii, but the $\sqrt{3}\times 700$ km s^{-1} relative velocity gives a much longer timescale of 2.5×10^{10} yr, longer than the age of the universe. Then, in Sersic 40/6 the presence of the core will not imply growth of the dumbbell. These numbers can vary somewhat depending on assumed $\mathscr{M}/L$ and luminosities for compact ellipticals. Brighter (more massive) galaxies should have faster decay rates; fainter, slower ones. The dependence on velocity is more complicated, but below a certain value, slower galaxies should be subjected to weaker friction. To analyze a possible correlation, we have plotted in Fig. 7 the galaxy magnitudes in the cores versus their velocities (relative to the db mean or cD velocity). Eye estimated magnitudes taken from Dressler (1980) have been used for A496 and photographic photometry magnitudes from Melnick and Quintana (1990) for Sersic 40/6. As can be seen, basically all the faster moving objects have brighter magnitudes than the slower ones. This is contrary to what may be expected from equipartition alone. The dynamical friction rate formula implies that frictional rates for faster galaxies should be stronger, i.e., they should be falling faster than fainter ones. One should keep in mind, however, that some high velocity galaxies should be just seen projected on the inner core, most on elongated orbits (Merritt 1983; Cowie and Hu 1986).

The presence in A496 and A2589 (Bothun and Schombert 1988) of bound cores to cD galaxies would indicate that perhaps more than 20% of the cluster mass is in galaxies, if we apply Merritt (1988) simulations. Core absence in the other clusters studied by Bothun and Schombert (1988) may, likewise, indicate that the fraction of matter in galaxies varies much from cluster to cluster. In fact, little is known on the mechanisms controlling galaxy efficiency formation and on the ratio of detectable to dark matter in clusters. According to Merritt (1983), the frictional decay rate depends on the cluster velocity dispersion, i.e., their total mass, and on the proportion of mass in galaxy form, thus being related to the efficiency of galaxy formation.

The presence of dynamical cusps in A496 and A2589 and their absence in other cD clusters suggest that ambigous results will be derived by studies of a composite of many dissimilar clusters,as Cowie and Hu (1986) have done.

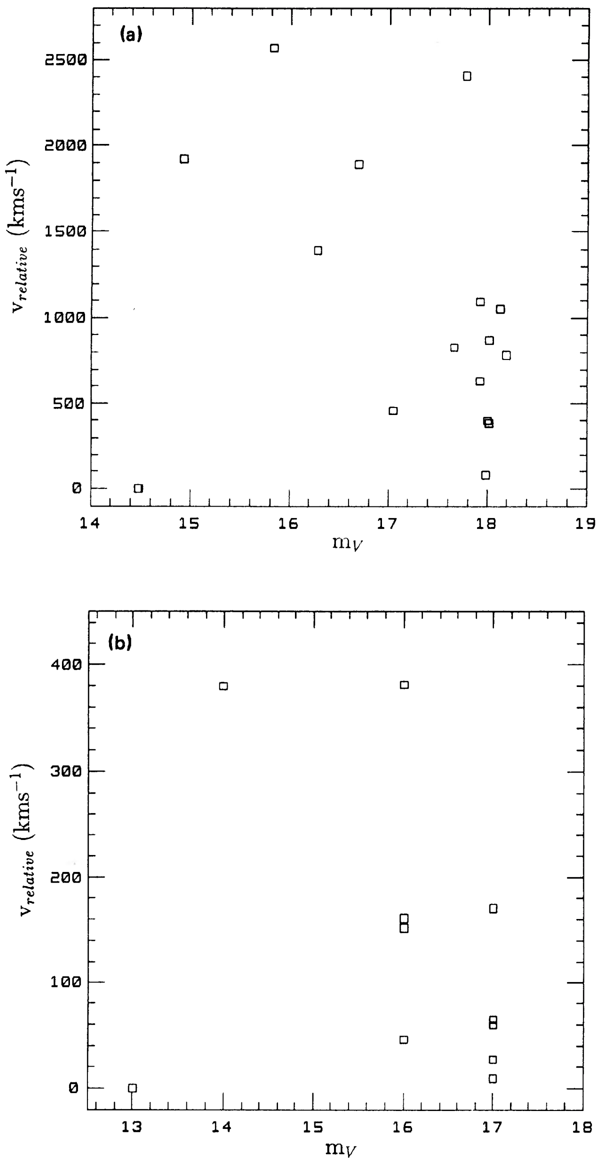

FIG. 7. (a) Velocities (relative to mean of db) for the 15 central galaxies in Sersic 40/6 as a function of magnitude. (b) Velocities (relative to cD) for the ten central galaxies in A496 as a function of magnitude.

Finally, we return to the case of Sersic 40/6. With a velocity dispersion of 1500 km s^{-1} the calculations of Merritt (1985) predict extremely long decay rates due to dynamical friction. No bound core could have been formed by this mechanism. The presence of a (bound?) central massive dumbbell complicates the analysis as the core potential will be markedly nonspherical and time variable. At face value, the 700 km s^{-1} core dispersion is very high. It is in fact comparable to the dispersions of whole clusters. There is a chance that the high global dispersion of 1500 km s^{-1} is just an artifact of a hidden superposition of an ensemble of groups belonging to a wider structure and that the cluster true dispersion is closer to 700 km s^{-1}. Only further data will settle this matter. The second alternative is that the core is indeed real; galaxies belong to a subunit. Whether a galaxy is bound to the central db or to the inner core is less relevant in this respect.

How could such a core have formed and evolved? Could the presence of a db have a dynamical effect? In fact, brightest db's in clusters still present a perplexing case. Calculations show that (isolated) massive db should coalesce rather quickly (of order 10^8 yr). However, there is a significant fraction of them at the centers of clusters (Rood and Leir 1979) that shows typical tidal distortions of close interacting systems (Valentijn and Casertano 1988). There are also many db's in the field that appear isolated or in poor groups. An observation that may bear on Sersic 40/6 is the measurement of the velocity dispersion of groups of faint galaxies apparently clustered around field dumbbells (De Souza and Quintana 1990; Quintana 1990). In the two cases studied so far, the virial theorem as well as other mass estimators, gives very large masses, of order $10^{14}\,\mathscr{M}_\odot$, for these poor systems. Thus they appear to contain large quantities of dark matter, either in halos originally bound to the individual db members or in a common halo with a size of order 300 kpc. The presence of large dark matter halos will increase merging times, as suggested by calculations on groups by Mamon (1990). We note here that the relative radial velocities in the two db studied are 650 km s^{-1} and 890 km s^{-1} (references cited), much higher than for typical bound pairs and the group dispersions are 450 and 700 km s^{-1}, respectively. Both db show strong tidal distortions so that a simple projection explanation for the high relative velocities can be rejected. If db galaxies contribute with an additional massive dark halo, perhaps the core galaxies in Sersic 40/6 settled around it during virialization, at the time of the formation of the db central galaxy. Then, the slow rates of decay are similar to the other groups around dumbbell galaxies. A detailed discussion of these several possibilities is out of the scope of this paper.

V. CONCLUSIONS

The main conclusions of this paper are as follows:

(1) We have confirmed the high velocity dispersion of 1440 km s^{-1} of Sersic 40/6, which implies a very large dynamical mass, $(3\pm1)\times10^{15}\,\mathscr{M}_\odot$ approximately, as calculated by different methods that assume a relaxed and bound system.

(2) We have confirmed the previously estimated low dispersion of 620 km s^{-1} for A496. A similarly derived dynamical mass gives an approximate value of $(5.5\pm1)\times10^{14}\,\mathscr{M}_\odot$.

(3) In both these two cD dominated clusters we found cores of galaxies close to the cD or db, which form density cusps and show low velocity dispersions (relative to the cluster value). In fact, these dispersion values smoothly join the stellar halo velocity dispersions of the central galaxies, indicating these cores are bound to the cD's and, as such, are dynamical subunits. Given the high values found for Sersic 40/6, this result would need confirmation from a wider velocity survey.

(4) Comparing to other clusters discussed in the literature, it seems that cores were formed in some cD clusters, but not in others. A study of the bound population from a composite of different clusters will be affected by that effect.

(5) The dynamical masses of central cores approximately are $(2.1\pm1.0)\times10^{14}\,\mathscr{M}_\odot$ for Sersic 40/6 and $(7.0\pm2.0)\times10^{12}\,\mathscr{M}_\odot$ in A496, with presumably most of the mass in the cD's. If one takes the very inner core around the A496 cD, one derives a cD mass of $\sim2.5\times10^{12}\,\mathscr{M}_\odot$. The very large mass of the db in Ser 40/6 is outstanding, giving about $10^{14}\,\mathscr{M}_\odot$ for each db component, at the top range of measured cD masses. As pointed out, this latter result would require further testing of the bound assumption of the central subunit.

(6) From the velocity data and density contours Sersic 40/6 appears to be a symmetric cluster where no projected groups can be distinguished. A496 shows some substructures in the NW region at 35′ from the cD seen in density and velocity data. It also shows a large elongation to the NW at large scales which may be due to obscuration produced by galactic nebulae.

(7) The presence of dynamical cores in the inner regions of clusters, showing much lower velocity dispersions than the clusters values, could be an important factor for the formation and evolution of cooling flows, which need to be taken into account.

A more detailed analysis, including further velocities and photometric data for both clusters, will be reported in future work.

We are pleased to acknowledge partial support from Grants No. 88/362 of FONDECYT and DIUC No. 86/38 of Pontificia Universidad Católica de Chile. We are thankful to the Directors of the Las Campanas Observatory and Cerro Tololo Inter-American Observatory for allocations of telescope time and to the Director General of the European Southern Observatory for support on a visit to Garching during which we used the OPTRONICS engine. We acknowledge the professional and friendly assistance of Fernando Peralta and Angel Guerra at the du Pont telescope. We thank an anonymous referee for comments that help improve the paper presentation.

REFERENCES

Abell, G. O., Corwin, H. G., and Olowin, R. P. (1989). Astrophys. J. Suppl. **70**, 1.

Abt, A., and Biggs, E. (1972). *Bibliography of Stellar Radial Velocities* (Latham Process Corp., New York).

Bahcall, J., and Tremaine, S. (1981). Astrophys. J. **244**, 805.

Binney, J., and Tremaine, S. (1987). *Galactic Dynamics* (Princeton University, Princeton).

Bontekoe, T. R., and van Albada, T. S. (1987). Mon. Not. R. Astron. Soc. **224**, 349.

Bothun, G. D., and Schombert, J. M. (1988). Astrophys. J. **335**, 617.

Bower, R. G., Ellis, R. S., and Efstathiou, G. (1988). In *Cooling Flows in Clusters and Galaxies*, edited by A. C. Fabian (Kluwer, Dordrecht), p. 115.

Carter, D., Inglis, I., Ellis, S., Efstathiou, G., and Godwin, J. G. (1985). Mon. Not. R. Astron. Soc. **212**, 471.

Carter, D., Teague, P. F., and Gray, P. M. (1984). In *Groups and Clusters of Galaxies*, edited by F. Mardirossian (Reidel, Dordrecht), p. 93.

Cooke, B., Ricketts, M., Maccacaro, T., Pye, J., Elvis, M., Watson, M., Griffiths, R., Pounds, K., McHardy, I., Maccagni, D., Seward, F., Page, C., and Turner, M. (1978). Mon. Not. R. Astron. Soc. **174**, 267.

Cowie, L. L., and Hu, E. M. (1986). Astrophys. J. **305**, L39.

Cowie, L. L., Hu, E. M., Jenkins, E. B., and York, D. G. (1983). Astrophys. J. **272**, 29.

Danese, L., de Zotti, G., and di Tullio, G. (1980). Astron. Astrophys. **82**, 322.

de Souza, R., and Quintana, H. (1990). Astron. J. **99**, 1065.

Dressler, A. (1980). Astrosphys. J. Suppl. **42**, 565.

Fabian, A., Ku, W., Malin, D., Mutshotzky, R., Nulsen, P., and Stewart, G. (1981). Mon. Not. R. Astron. Soc. **196**, 35.

Forman, W., Jones, C., Cominsky, L., Julien, P., Murray, S., Peters, G., Tananbaum, H., and Giacconi, R. (1978). Astrophys. J. Suppl. **38**, 357.

Green, M. R., Godwin, J. G., and Peach, J. V. (1988). Mon. Not. R. Astron. Soc. **234**, 1051.

Heisler, J., Tremaine, S., and Bahcall, J. (1985). Astrophys. J. **298**, 8.

Hernquist, L., and Weinberg, M. D. (1989) Mon. Not. R. Astron. Soc. **238**, 407.

Hu, E., Cowie, L., and Wang, Z. (1985). Astrophys. J. Suppl. **59**, 447.

Kowalski, M., Ulmer, M., Cruddace, R., and Wood, K. (1984). Astrophys. J. Suppl. **56**, 403.

Mamon, G. (1990). In *Paired and Interacting Galaxies*, IAU Colloquium No. 124, edited by J. Sulentic (NASA, Washington, DC).

Materne, J., Chincarini, G., Tarenghi, M. and Hopp, U. (1982). Astron. Astrophys. **109**, 238.

Mazure, A., Gerbal, D., Proust, D., and Capelato, H. V. (1986). Astron. Astrophys. **157**, 159.

Melnick, J., and Quintana, H. (1981a). Astron. Astrophys. Suppl. **44**, 87.

Melnick, J. and Quintana, H. (1981b). Astron. J. **86**, 1567.

Melnick, J. and Quintana, H. (1990). Unpublished.

Merrit, D. (1983). Astrophys. J. **264**, 24.

Merrit, D. (1985). Astrophys. J. **289**, 18.

Merrit, D. (1988). In *The Minnesota Lectures on Clusters of Galaxies and Large-Scale Structures*, edited by J. M. Dickey (ASP Conference Series) (Brigham Young University Print Services, Provo, UT), Vol. 5.

Nulsen, P. E. J., Stewart, G. C., Fabian, A. C., Mushotzky, R. F., Holt, S. S., Ku, W. H-M, and Malin, D. F. (1982). Mon. Not. R. Astron. Soc. **199**, 1089.

Proust, D., Talavera, A., Salvador Sole, E., Mazure, A., and Capelato, H. V. (1987). Astron. Astrophys. Suppl. **67**, 57.

Quintana, H. (1990). In *Paired and Interacting Galaxies*, IAU Colloquium No. 124, edited by J. Sulentic (NASA, Washington, DC).

Quintana, H., and Lawrie, D. (1982). Astron. J. **87**, 1.

Quintana, H., and Melnick, J. (1982). Astron. J. **87**, 972.

Quintana, H., Melnick, J., Infante, L., and Thomas, B. (1985). Astron. J. **90**, 410.

Rood, H. J., and Leir, L. (1979). Astrophys. J. Lett. **231**, L3.

Sandage, A. (1979). Astron. J. **83**, 904.

Sandage, A., and Tammann, G. A. (1981). *A Revised Shapley–Ames Catalog of Bright Galaxies* (Carnegie Institution of Washington, Washington, DC).

Schechter, P. (1976). Astrophys. J. **203**, 197.

Shectman, S. (1981). *Annual Report of the Director of Mount Wilson and Las Campanas Observatories 1980–1981* (Carnegie Institution of Washington, Washington, DC), p. 52.

Stone, R. S. P., and Baldwin, J. A. (1983). Mon. Not. R. Astron. Soc. **204**, 347.

Tonry, J. (1985). Astron. J. **90**, 2431.

Valentijn, E. A., and Casertano, S. (1988). Astron. Astrophys. **206**, 27.

Vidal, N. (1975). Publ. Astron. Soc. Pac. **87**, 625.

West, R. M., and Frandsen, S. (1980). Astron. Astrophys. Suppl. **44**, 327.

Wood, K. S., Meekins, J. F., Yentis, D. J., Smathers, H. W., McNutt, N. P., Bleach, R. D., Byran, E. T., Chubb, T. A., Friedman, H., and Meidav, M. (1984). Astrophys. J. Suppl. **56**, 507.

Yahil, A., and Vidal, N. (1977). Astrophys. J. **214**, 347.

Zavitsky, D., and White, S. D. M. (1988) Mon. Not. R. Astron. Soc. **235**, 289.

Zavitsky, D., and White, S. D. M. (1988) Mon. Not. R. Astr. Soc. **235**, 289.